Localization and anchoring of mRNA in budding yeast

Dale L. Beach, E.D. Salmon and Kerry Bloom

Background: Eukaryotic cells localize selected mRNAs to a region of the cell as a means to sequester proteins. Signals within the 3′ untranslated region (3′UTR) facilitate mRNA localization by both actin and microtubule cytoskeletal systems. Recently, an mRNA in the yeast *Saccharomyces cerevisiae, ASH1*, was shown to coalesce into a discrete particle that is maintained at the bud tip. Mutations in five genes, *SHE1–SHE5*, cause defects in particle formation and/or localization of the *ASH1* transcript. Factors at the destination of the mRNA transport remain to be identified.

Results: We have developed a system to label mRNA in living yeast with green fluorescent protein (GFP) and follow the dynamics of mRNA movement and localization. Constitutively expressing an *ASH1* mRNA containing the bacteriophage MS2 coat-protein binding site adjacent to the *ASH1* 3′UTR allowed us to visualize *ASH1* mRNA with an MS2-coat-protein–GFP fusion protein (together denoted 'gRNA$_{ASH1}$'). The gRNA$_{ASH1}$ was restricted to the bud tip in small to large budded cells, migrated to the bud neck prior to cell separation and then rapidly relocalized to the incipient site of bud growth. It also localized to regions of polarized growth during mating. In cells lacking Bud6p/Aip3p or Bni1p/She5p, which are involved in polarity establishment and actin organization, gRNA$_{ASH1}$ migrated to the bud but failed to remain at the bud tip. These studies reveal discrete transport and anchoring steps in mRNA localization.

Conclusions: The *ASH1* mRNA was maintained at sites of polarized growth throughout the vegetative and mating cell cycles. Bud6p/Aip3p and Bni1p/She5p are required to maintain the transcript at the cortical bud cap.

Address: Department of Biology, University of North Carolina, 212 Coker Hall CB3280, Chapel Hill, North Carolina 27599-3280, USA.

Correspondence: Kerry Bloom
E-mail: Kerry_Bloom@unc.edu

Received: 9 November 1998
Revised: 12 April 1999
Accepted: 13 April 1999

Published: 19 May 1999

Current Biology 1999, 9:569–578
http://biomednet.com/elecref/0960982200900569

 ISSN 0960-9822

Background

Eukaryotic cells have developed several mechanisms to segregate proteins to structural and functional regions of the cell. One method is to spatially limit translation of the mRNA encoding the protein. The localization of mRNA within a cell is a dynamic process in which mRNA is subject to directed transport and maintenance at a specified location within the cell. In yeast, Ash1p is a cell-fate determinant that inhibits transcription of the gene encoding the HO endonuclease and blocks mating-type interconversion in the daughter cell [1,2]. Asymmetric localization of Ash1p is brought about by *SHE1–SHE5*-dependent localization of *ASH1* mRNA to the bud tip [3–5], thereby restricting protein synthesis to the daughter cell. *Cis*-acting signals within the 3′ untranslated region (3′UTR) of *ASH1* mRNA are recognized by specific target molecules that are required for its nuclear export and localization [6,7]. *SHE2–SHE4* appear to be required for the formation of an *ASH1* mRNA particle before transport [4], whereas transit and positioning of the particle relies upon *MYO4*/*SHE1* and *BNI1*/*SHE5* in association with the actin cytoskeleton. Finally, it is likely that predetermined sites in the cortical bud cap are marked as the destination of the transport step.

Transport and anchorage of mRNA is a good example of a dynamic cellular process that is amenable to live-cell analysis. Previous examples of real-time imaging of RNA movements in cells have required injection of labeled RNA [8] or RNA-specific dye [9]. The advent of green fluorescent protein (GFP)-fusion proteins has allowed the visualization of highly dynamic processes and has been invaluable in assessing the functional attributes of a given protein. We describe a novel system that uses a cytoplasmic RNA-binding protein fused to GFP to visualize a small RNA transcript containing the specific binding site for the RNA-binding protein. Coexpression of the two parts of this RNA-labeling system allows direct visualization of RNA dynamics in live cells by digital imaging microscopy of GFP fluorescence [4].

Our live-cell studies reveal that *ASH1* mRNA is anchored to cortical sites near the bud tip in vegetative cells as well as near the mating projection during karyogamy (fusion of haploid nuclei upon mating). These cortical regions are spatially coincident with factors that are required for accurate establishment of polarity and organization of the actin cytoskeleton. *ASH1* mRNA polarization requires myosin for its transport [4]. Two proteins, Bni1p/She5p and

Bud6p/Aip3p, are required for docking of *ASH1* mRNA at the bud tip. The actomyosin-dependent transport of the *ASH1* mRNA into the bud, together with the docking mechanism, is essential in generating the highly asymmetric distribution of *ASH1* mRNA *in vivo*.

Results

RNA-labeling system

The GFP-labeling system for RNA is shown in Figure 1. The bacteriophage-MS2 coat protein (CP) binds RNA transcripts that contain the CP-binding site in both *Escherichia coli* [10] and yeast [11]. Expression of a CP–GFP fusion protein with an RNA containing the 23 bp CP-binding site resulted in fluorescently labeled RNA, which we denote gRNA. The system described here is similar to that described by Bertrand and coworkers [4]. We used a regulated cytoplasmic CP–GFP that can be attenuated to visualize gRNA without high levels of background fluorescence. This feature allowed visualization of nuclear retention and export of gRNA, which is not possible with the previous system. Additionally, the reporter RNA in this system contains only two CP-binding sites, which proved sufficient to visualize the mRNA and reduce potential problems with increased 3′UTR length.

To demonstrate the efficacy of the system, we examined a nuclear-localized RNA ($gRNA_{NUC}$), expressed from the vector pIIIA/MS2-1 (see Materials and methods). The nucleus can be visualized by differential interference contrast (DIC) microscopy [12] and exhibits discrete morphological changes throughout the cell cycle [12]. The $gRNA_{NUC}$, visualized by time-lapse digital fluorescent microscopy [13], was restricted to the nucleus throughout the cell cycle (Figure 2a). To verify that expression of the CP–GFP and the RNA transcript did not adversely affect the cell, we examined morphological changes and the rate of spindle elongation. The usual transitions from sausage-shaped to bilobed nuclear structures were evident, and the rate of nuclear elongation during anaphase was 0.33 ± 0.17 μm/minute (n = 4), the same as the slow phase of elongation that has been measured by DIC in budding yeast [12]. Expression of CP–GFP in the absence of an RNA component produced an amorphous distribution of fluorescence throughout the cell. CP–GFP was excluded only from the vacuole and no punctate spots were visible (Figure 2c).

Imaging $gRNA_{ASH1}$ localization and movement in live cells

We used the 3′UTR of *ASH1* mRNA to visualize an asymmetrically localized transcript. The 3′UTR of the *ASH1* mRNA contains information for the localization of *ASH1* mRNA to the bud tip [3,4,14] and was used to construct $gRNA_{ASH1}$ (see Materials and methods). Other regions of the *ASH1* coding region can also direct localization of the mRNA [15,16]. Using a single region from the *ASH1* transcript for localization generates a reporter RNA that is highly sensitive (or 'sensitized') to effectors acting on the *ASH1* 3′UTR.

Figure 1

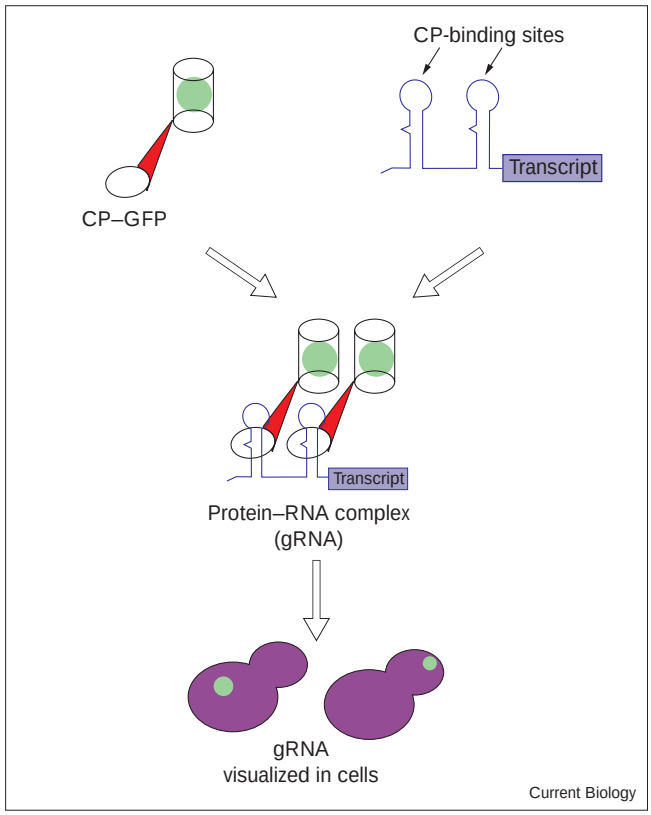

The RNA-labeling system contains two components: the RNA-binding MS2 coat protein (CP) fused to GFP, and an RNA transcript containing the CP-binding site. The CP-binding sites can be fused to all or part of a transcript to be studied. When coexpressed in the cell, the components interact to form a GFP-labeled RNA (gRNA), which can be visualized using common fluorescence microscopy techniques, as shown for a nuclear-localized RNA (bottom left) and for an mRNA localized to the bud tip (bottom right).

The $gRNA_{ASH1}$ construct was expressed from a constitutive promoter throughout the cell cycle and was visible as an asymmetrically localized, highly motile spot of fluorescence in the bud tip of large budded cells (Figures 2b,3). Asymmetric localization of $gRNA_{ASH1}$ to the bud tip was confirmed by using fluorescence *in situ* hybridization (FISH) to label the reporter transcript in the absence of the CP–GFP (see the Supplementary material published with this paper on the internet). The observed localization of $gRNA_{ASH1}$ in live cells was consistent with previous studies that demonstrated *ASH1* mRNA localization to the bud tip in fixed cells using FISH [3,14] and a similar method to label mRNA with GFP [4].

The 3′UTR region of *ASH1* was essential for nuclear export and asymmetric distribution of *ASH1* mRNA.

When the *ASH1* 3′UTR was placed in the opposite orientation such that the noncoding sequence was transcribed ($gRNA_{NONCODING}$), the reporter RNA remained within the nucleus throughout the cell cycle (Figure 2d). Thus, information in the 3′UTR was sufficient to promote export of *ASH1* mRNA from the nucleus. To address the specificity in RNA positioning by the *ASH1* 3′UTR, we examined the ability of the 3′UTR of *KAR9* to localize RNA. Kar9p has recently been found to localize to the bud tip in large budded cells, where it is presumably involved, in conjunction with dynein and other molecules, in directing spindle orientation and nuclear migration during anaphase [17,18]. We constructed $gRNA_{KAR9}$ by placing the 3′UTR of *KAR9* downstream of the two CP-binding sites of the reporter RNA (see Materials and methods). The $gRNA_{KAR9}$ was exported from the nucleus and produced a punctate distribution of GFP spots smaller than those seen for $gRNA_{ASH1}$ ($n = 3$; data not shown). The speckles were highly motile, but there was no organized subcellular distribution (data not shown). Likewise, FISH images of total polyadenylated RNA within yeast cells show a general staining in the cytoplasm [3]. Localization to the bud tip was therefore a function specific to the *ASH1* 3′UTR.

Live-cell time-lapse images revealed dramatic cell-cycle-dependent movements of $gRNA_{ASH1}$. Large budded cells displayed localized foci of $gRNA_{ASH1}$ at the cortical region of the bud tip (Figure 3a). As the bud grew, the $gRNA_{ASH1}$ moved within 0.3 μm of the tip (Figure 3b,h and see later graph). We denote this region of the bud tip the 'cortical bud cap'. The $gRNA_{ASH1}$ spot migrated to the mother and daughter sides of the bud neck 20 ± 5 minutes ($n = 4$) before cell separation (Figure 3c,d). Small movements of around 0.2 μm occurred while the $gRNA_{ASH1}$ was at the neck, and in some cases $gRNA_{ASH1}$ spots on the mother and daughter sides of the neck moved independently from each other. The $gRNA_{ASH1}$ migrated to the incipient bud site 10 minutes before cell separation, as seen by lateral movement in Figure 3d,e. The emerging bud contained $gRNA_{ASH1}$ at the cortical cap (Figure 3g,h). These cell-cycle changes in localization were verified by detection of the reporter transcript by FISH in the absence of CP–GFP expression (see Supplementary material).

Two types of $gRNA_{ASH1}$ with differing velocities were identified. The $gRNA_{ASH1}$ moved at a rate of 1.99 μm/minute ($n = 2$) over the long-distance translocation from cortical cap to neck (Figure 3b,c and see later graph), whereas the short-range movement that was confined to the cap (Figure 3a,b and see later graph) had an average velocity of 0.307 μm/minute (range 0.069–1.02 μm/minute; $n = 8$). Short-range movements also occurred at the neck and incipient bud site (Figure 3e,f) averaging 0.109 μm/minute (range 0.079–0.176 μm/minute; $n = 8$). We have thus identified short-range movements of the $gRNA_{ASH1}$ when juxtaposed to the cortical cap or the neck.

Figure 2

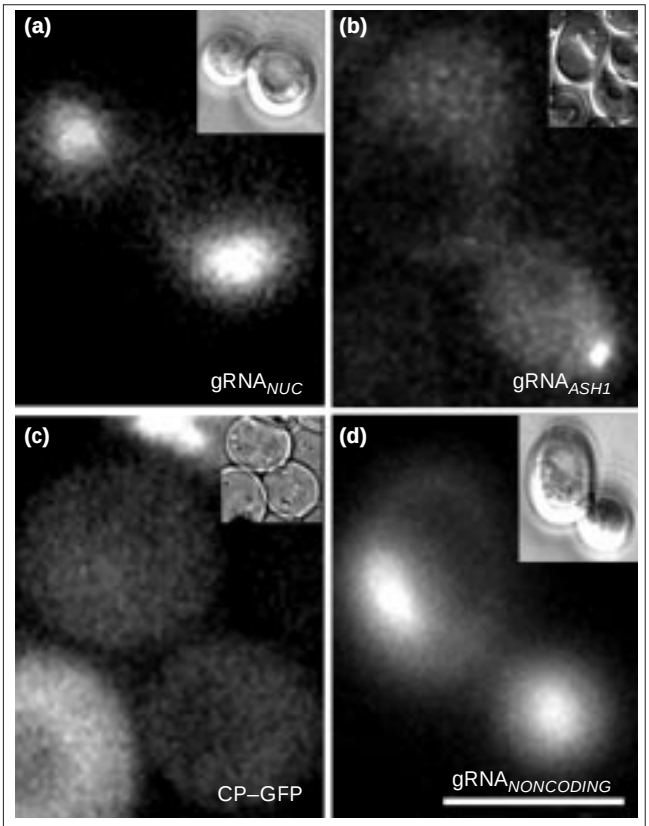

The *ASH1* 3′UTR is necessary and sufficient for nuclear export and localization of the *ASH1* mRNA. (a) The $gRNA_{NUC}$ produced from the plasmid pIIIA/MS2-1 contains two CP-binding sites flanked by the 5′ leader sequence and the 3′ terminator of the RNAse P RNA component. This RNA remains within the nucleus (see text) and is fluorescently labeled when coexpressed with the CP–GFP. The GFP fluorescent image shows a large budded, post-anaphase cell containing two nuclei separated between mother and bud cellular compartments ($n = 6$). (b) We generated $gRNA_{ASH1}$ by placing the *ASH1* 3′UTR downstream of the CP-binding sites of $gRNA_{NUC}$. Coexpression of $gRNA_{ASH1}$ and CP–GFP produces a spot of GFP fluorescence at the tip of large budded cells, and does not label the nucleus ($n = 10$). (c) Expression of CP–GFP without a reporter transcript containing the CP-binding site results in a uniformly labeled cytoplasm excluding only the vacuole. The field of view shows a large budded cell with low levels of fluorescence (center) and flanking cells with higher levels (top and bottom) typical in a population. (d) The $gRNA_{NONCODING}$ contains the *ASH1* 3′ UTR oriented such that the noncoding strand is transcribed. The presence of two labeled nuclei in the GFP image of a large budded, post-anaphase cell demonstrates the expected nuclear retention of the RNA ($n = 4$). Insets show the orientation of the cells in the fluorescence images. The scale bar represents 5 μm.

Relocation required a long-range transit associated with a sixfold increase in velocity of the $gRNA_{ASH1}$.

The $gRNA_{ASH1}$ is localized to mating projections

Upon exposure to mating pheromones, yeast cells arrest in G1 and a mating projection or 'shmoo' forms [19].

Figure 3

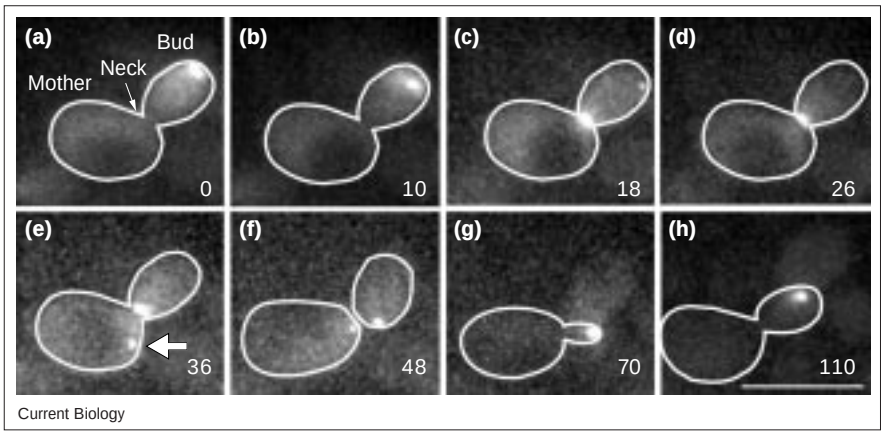

Sequential time-lapse images showing the position of gRNA$_{ASH1}$ within a haploid cell through the cell cycle. The white borders, obtained from transmitted light images, outline the cell surface, and the mother, neck, and bud regions are indicated. (a) A large budded cell with a single gRNA$_{ASH1}$ spot at the bud tip. (b) gRNA$_{ASH1}$ transiently exhibits short-range movements away from the extreme tip of the bud. (c) Prior to cytokinesis, the gRNA$_{ASH1}$ relocates to the bud neck. A small amount remains near the bud tip. (d) Migration of the gRNA$_{ASH1}$ to the neck is complete. (e) A portion of the gRNA$_{ASH1}$ relocates to the incipient site of bud growth (arrow). (f) After cell separation has occurred at 46 minutes, both mother and bud retain gRNA$_{ASH1}$ signal. (g) The growing bud harbors gRNA$_{ASH1}$ at the bud cap. The daughter cell has moved out of focus in this image. (h) The bud has grown large, and gRNA$_{ASH1}$ maintains mobility at the bud tip (n = 10). Elapsed time is indicated for each frame in min. The scale bar represents 5 μm.

Positioning of the mating projection represents polarized cell growth in response to extrinsic signals. Many of the proteins that are involved in polarity establishment, actin organization, and bud-site selection in vegetative cells also localize to the shmoo tip during mating [20–22]. The continued maintenance of *ASH1* mRNA localization throughout the cell cycle that we found implied that mechanisms responsible for positioning the mRNA would persist in mating as well. If putative anchoring mechanisms were constitutively available, then expression of gRNA$_{ASH1}$ in mating cells would result in gRNA$_{ASH1}$ localization at the tip of the mating projection. Haploid cells expressing gRNA$_{ASH1}$ (YEF473A; *MAT***a**) were treated with the mating pheromone α factor for 3 hours to induce mating projection formation. Within the population of cells exhibiting mating projections, 44% contained gRNA$_{ASH1}$ within the shmoo or at the shmoo tip, 5% contained gRNA$_{ASH1}$ only within the cell body, and the remaining 51% contained no visible spots of fluorescence (n = 95).

Figure 4

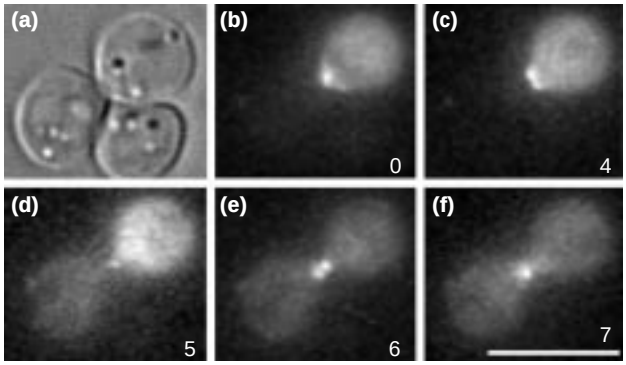

The gRNA$_{ASH1}$ localizes to the shmoo tip in mating cells (n = 2). (a) A bright-field image of two mating cells (upper-right and left-most cells). (b,c) Before cell fusion, the gRNA$_{ASH1}$ is located at the intersection of the two cells at the tip of the mating projection (shmoo), and the GFP fluorescence is limited to the upper-right cell, which produces gRNA$_{ASH1}$. (d–f) Once the cells fuse, the cytoplasms mix such that both cells now contain GFP fluorescence. (e) After cell fusion, two bands of gRNA$_{ASH1}$ appear between the two cells followed by (f) resumption of dynamic movement of gRNA$_{ASH1}$ within the isthmus. (b–f) Elapsed time is indicated for each frame in min. The scale bar represents 5 μm.

When the same strain was combined with *MAT*α cells (YEF473B), mating commenced and cell fusion occurred within 3 hours. The gRNA$_{ASH1}$ was seen at the isthmus between the two mating cells prior to cell fusion (Figure 4b,c). Transfer of cytoplasmic fluorescence from a cell expressing CP–GFP into a non-expressing partner indicated the onset of cell fusion (Figure 4d). After fusion, the gRNA$_{ASH1}$ remained dynamic, moving within the isthmus between the two cells (Figure 4d–f). This result demonstrated that the gRNA$_{ASH1}$ could be localized to regions of polarized growth during both vegetative and mating cell cycles.

Determinants of *ASH1* mRNA polarity and anchoring

Myo4p/She1p is one of the two class-V myosin motors in yeast [23]. In *myo4/she1* mutant cells, as in wild-type cells, gRNA$_{ASH1}$ coalesced into visible spots (Figure 5b). Unlike in wild-type cells, however, gRNA$_{ASH1}$ did not localize to the bud tip, neck or incipient bud site. A discrete spot was visible in the mother of small budded cells (Figure 5a,b), and in both mother and bud of large budded cells. Although the gRNA$_{ASH1}$ remained in the mother, the spot was still dynamic. Movements of gRNA$_{ASH1}$ spots in the *myo4/she1* mutant strain were similar to the short-range

Figure 5

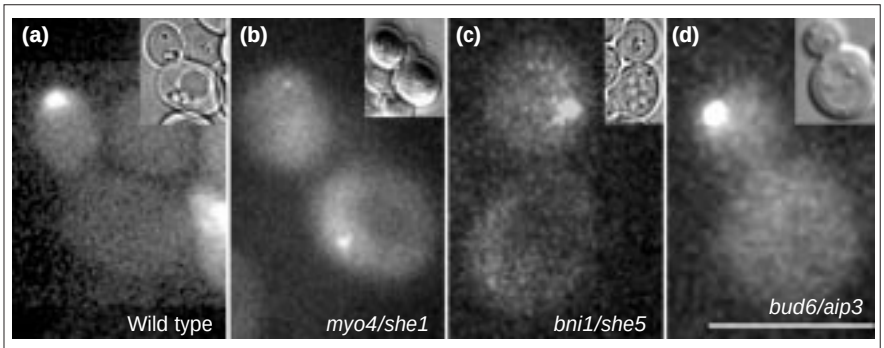

The appearance and localization of $gRNA_{ASH1}$ in wild-type, *myo4/she1*, *bni1/she5* and *bud6/aip3* mutant cells. (a) In a wild-type cell, the $gRNA_{ASH1}$ is localized to the cortical bud tip. (b) In *myo4/she1* cells, $gRNA_{ASH1}$ is in an unbudded cell (upper left) and the mother of a small budded cell (lower right; bud growth is up, $n = 4$). No $gRNA_{ASH1}$ was ever observed in small buds of *myo4/she1* mutants. In *bni1/she5* cells, $gRNA_{ASH1}$ is polarized to the bud, but is not restricted to the cortical bud cap as was seen in wild-type cells ($n = 4$). (d) The $gRNA_{ASH1}$ is polarized to the bud and resides within the cortical bud cap in this frame of the *bud6/aip3* time-lapse ($n = 3$). Transmitted light images of the cells are shown in the inset. The scale bar represents 5μm.

movements seen in wild-type cells at the neck and cortical cap. Velocities of the $gRNA_{ASH1}$ movements averaged 0.629 μm/minute (range 0.142–2.12 μm/minute; $n = 25$).

In order to display the range of movement of the $gRNA_{ASH1}$ in the *myo4/she1* mutant, we generated a composite image showing the distribution of the $gRNA_{ASH1}$ in the cell with time. Ten sequential images of a wild-type cell, and ten from a *myo4/she1* cell, were combined into single images (Figure 6; see Materials and methods). The composite image for the wild-type cell showed $gRNA_{ASH1}$ predominantly at the cortical cap and at the neck. The composite for the *myo4/she1* cell revealed $gRNA_{ASH1}$ scattered exclusively within the body of the mother, which indicates RNA motility in the absence of Myo4p/She1p. These results point to an alternative source of locomotion or a lack of anchorage to maintain position in the absence of Myo4p/She1p.

Bni1p/She5p is a member of the class of proteins containing formin homology domains. Mutants of *bni1/she5* exhibit slight defects in actin organization, are defective in bud-site selection in diploid cells and are unable to form mating projections [24,25]. Bni1p/She5p is localized to the bud tip in small budded cells and the neck late in the cell cycle [5,24]. Mislocalization of *ASH1* mRNA in *bni1/she5* mutants [3,4,14] implicated Bni1p/She5p as a potential mRNA anchor in the bud. In the *bni1/she5* cells, $gRNA_{ASH1}$ was asymmetrically localized to the bud, but was not maintained at the cortical bud cap (Figure 5c). The $gRNA_{ASH1}$ moved throughout the bud (1.5–2 μm from the bud tip; Figures 6,7), a much greater distance than the 0.3 μm excursions from the bud tip in wild-type cells. Thirty minutes before cell division, the $gRNA_{ASH1}$ returned to the bud neck. In order to display the range of movement of the $gRNA_{ASH1}$ in the *bni1/she5* mutant, we generated a time-lapse composite of 10 sequential images of *bni1/she5* cells taken at 1 minute intervals (Figure 6c). The composite for the *bni1/she5* cell showed $gRNA_{ASH1}$ scattered throughout the bud, with no fluorescence in the mother cell. In medium- to large-sized buds, the $gRNA_{ASH1}$ was highly motile, moving at an average velocity of 0.467 μm/minute (range 0.064–3.273 μm/minute; $n = 77$). From these observations, we concluded that

Figure 6

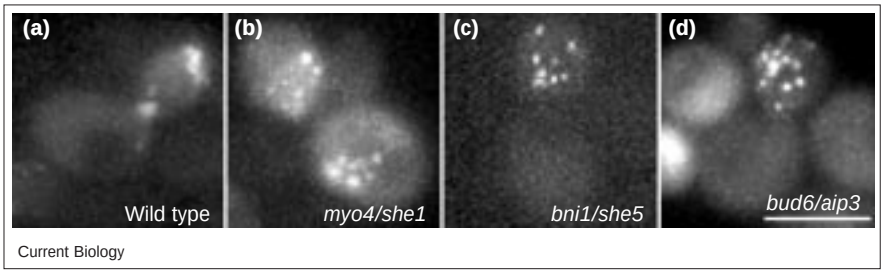

Ten sequential time-lapse images for (a) wild-type, (b) *myo4/she1*, (c) *bni1/she5* and (d) *bud6/aip3* cells were combined to form a single composite image showing the $gRNA_{ASH1}$ position. (a) Wild-type cells maintained $gRNA_{ASH1}$ at the cortical bud cap until migration to the bud neck. (b) In *myo4/she1* cells, the $gRNA_{ASH1}$ remains motile within the mother domain of a small budded cell (lower right; a small bud extends upward, as in Figure 5b) and an unbudded cell (upper left) as indicated by the distribution of fluorescent spots within the cell. (c,d) In *bni1/she5* and *bud6/aip3* cells, $gRNA_{ASH1}$ was restricted to the bud but was not anchored to the cortical bud cap and moved throughout the bud. The elapsed time for wild type was 20 min; for *myo4/she1*, 10 min; for *bni1/she5*, 10 min; and for *bud6/aip3*, 10 min. The scale bar represents 5 μm.

Figure 7

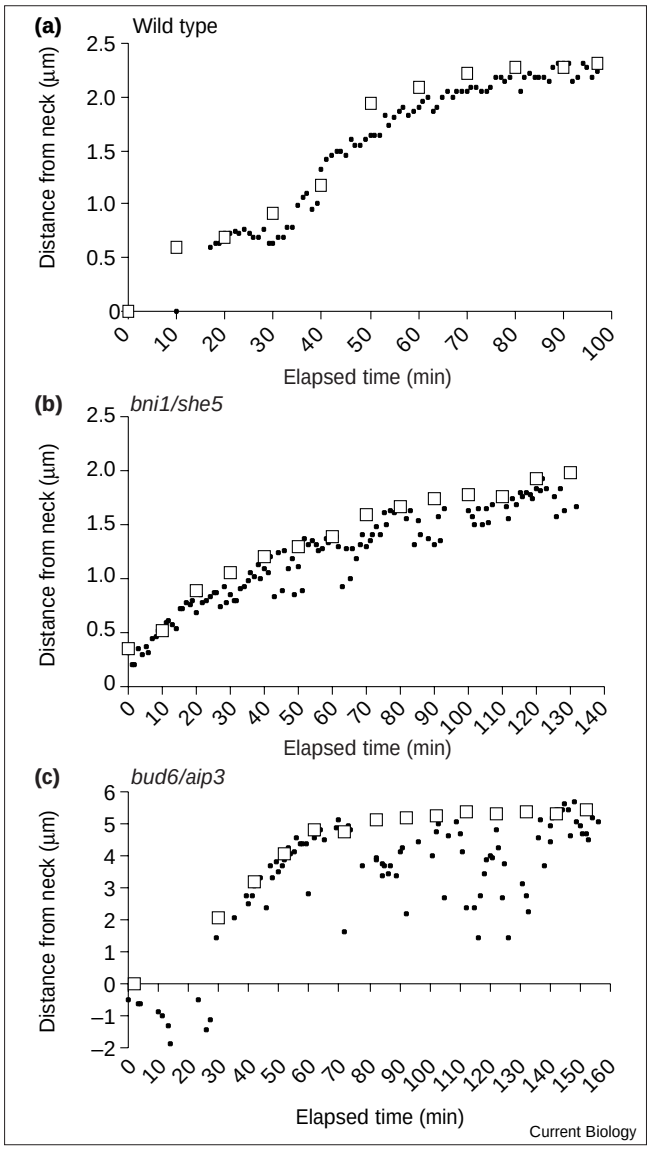

Neck to bud tip (open squares) and neck to gRNA$_{ASH1}$ spot (black dots) distances were measured in time-lapse images of (a) wild-type, (b) *bni1/she5* and (c) *bud6/aip3* strains expressing gRNA$_{ASH1}$, then plotted against elapsed time. (a) In wild-type cells, the bud tip and gRNA$_{ASH1}$ distances from the neck are similar, showing that gRNA$_{ASH1}$ remains associated with the bud tip throughout the cell cycle. (b,c) In *bni1/she5* and *bud6/aip3* cells, the distance from the neck to bud tip is frequently greater than the neck to gRNA$_{ASH1}$ distance, suggesting that the gRNA$_{ASH1}$ is not tightly bound to the bud tip. Negative neck to gRNA$_{ASH1}$ values in (c) indicate gRNA$_{ASH1}$ within the mother cell. The y-axis differences between the graphs result from a twofold larger bud in *bud6/aip3* cells.

Bni1p/She5p is required to maintain *ASH1* mRNA at the cortical cap, but is not required for polarized translocation from mother to bud.

Bud6p/Aip3p is another protein required for bipolar bud-site selection and organization of the actin cytoskeleton, and it directly binds both actin and Bni1p/She5p [25,26]. We therefore used gRNA$_{ASH1}$ to examine potential defects in *ASH1* mRNA localization in *bud6/aip3* mutants. Spots of gRNA$_{ASH1}$ were asymmetrically localized to the bud, but were not maintained within the cortical cap (Figure 5d). The gRNA$_{ASH1}$ moved throughout the bud (more then 4 μm away from the cortical cap; Figure 7) and migrated to the neck by 20 minutes before cell separation (data not shown). The gRNA$_{ASH1}$ moved throughout the bud at an average velocity of 0.868 μm/minute (range 0.142–4.48 μm/minute; n = 121). After cell separation and before bud emergence, the gRNA$_{ASH1}$ moved throughout the new daughter cell at an average velocity of 0.990 μm/minute (range 0.211–3.48 μm/minute; n = 17). This movement in the unbudded cell did not occur in wild-type cells. The gRNA$_{ASH1}$ was delayed in entering the bud until approximately 4–30 minutes after bud emergence (see Figure 7c; range 0–29 minutes, n = 2). A time composite of *bud6/aip3* showed gRNA$_{ASH1}$ scattered throughout the bud and absent from the mother cell, as observed for *bni1/she5* cells (Figure 6).

The distances from the neck to the bud tip and from the neck to the gRNA$_{ASH1}$ spot were measured for wild-type, *bni1/she5* and *bud6/aip3* cells to quantify the frequency and distance of gRNA$_{ASH1}$ movements (Figure 7). In a wild-type cell, the gRNA$_{ASH1}$ and the bud tip overlapped for most of the cell cycle (within 0.3 μm). This confirmed the observation that the gRNA$_{ASH1}$ is maintained at the cortical cap. In both *bni1/she5* and *bud6/aip3* cells, the gRNA$_{ASH1}$ was displaced from the bud tip, such that the tip-to-spot distance was greater than half the bud length (53% and 80% of the bud length for *bni1/she5* and *bud6/aip3* cells, respectively; see Figure 7). The gRNA$_{ASH1}$ made excursions out of the 0.3 μm region of the cortical cap for only 9% of the time points in the wild-type cell. In contrast, the gRNA$_{ASH1}$ was outside the 0.3 μm range of the cortical cap for 28% of *bni1/she5* and 40% of *bud6/aip3* time points. Bni1p/She5p and Bud6p/Aip3p are thus required for maintaining the *ASH1* mRNA within the cortical bud cap but not for polarization of the mRNA.

Motility of Bud6p/Aip3p–GFP

Bud6p/Aip3p localizes to the tip of the bud during bud growth, migrates to the neck region before cytokinesis — forming two rings between the mother and bud — and then moves to the incipient site of bud growth [26] in a fashion remarkably similar to that described above for gRNA$_{ASH1}$. We imaged Bud6/Aip3p–GFP in our strains to obtain qualitative and quantitative measurements of the types and rates of Bud6p/Aip3p–GFP motility. Figure 8 shows three cells, two at a late stage of the cell cycle indicated by the large bud size, and the third early in the cell cycle, as indicated by the small bud. Whereas the spots of Bud6p/Aip3p–GFP fluorescence remained within the bud during bud growth, our images showed them to be spread

Figure 8

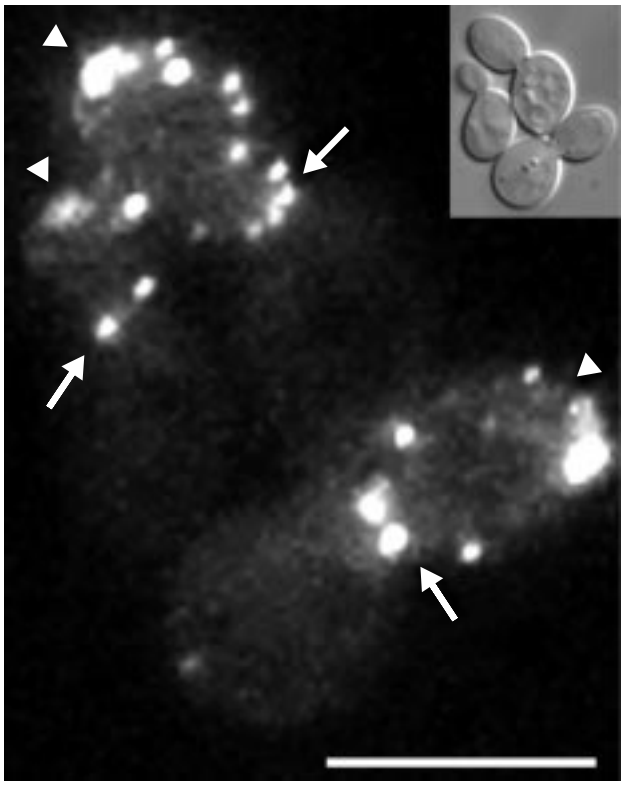

Localization of Bud6p/Aip3p–GFP within the growing bud of haploid cells. Fluorescent spots of Bud6p/Aip3p–GFP are apparent throughout the cortex of the bud, as well as at the bud tip (arrowhead) and neck (arrow). Three cells are shown at different points in the cell cycle, indicated by differential bud size. A fraction of Bud6p persists at the bud neck throughout the cell cycle. The scale bar represents 5 μm.

throughout the cortex (Figure 8). Prior to cell separation, Bud6p/Aip3p–GFP migrated from the tip region to the neck (20 minutes before separation for the upper cell, 23 minutes before for the left cell, and 26 minutes before for the lower cell of Figure 8; see also [26]).

Bud6p/Aip3p–GFP spot movements were analyzed by single-particle tracking in order to determine the migration velocities. Six spots from two buds were selected at random and found to move at an average velocity of 0.116 μm/minute (range 0.101–0.130 μm/minute). The Bud6p/Aip3p–GFP spots moved an average of 0.27 μm around a central point, such that over time there was no net migration. Thus, before moving to the neck, Bud6p/Aip3p–GFP particles remained confined to a small domain. During the migration towards the neck that preceded cell separation, Bud6p/Aip3p–GFP motility increased in speed to 0.621 μm/minute ($n = 4$). This represented a fivefold increase in the velocity for a particle moving towards the neck over those in the bud tip. Both $gRNA_{ASH1}$ and Bud6p/Aip3p–GFP exhibited similar velocities when restricted to the cap, and both increased in velocity upon migrating to the neck.

Discussion

We have designed a novel system to label mRNA within living yeast cells. Coexpressing a GFP-labeled RNA-binding protein with RNA containing the specific binding site generated a fluorescently labeled mRNA. Inclusion of the *ASH1* 3′UTR into the transcript to give $gRNA_{ASH1}$ and constitutive expression of the reporter RNA allowed detection of $gRNA_{ASH1}$ at specific sites within the cell throughout the cell cycle. The $gRNA_{ASH1}$ was localized to sites of polarized growth in budded cells and migrated back to the neck before cell division. Transport of *ASH1* mRNA from the nucleus to the bud was dependent upon *MYO4*/*SHE1* (Figures 5,6) [3,4,14]. Velocities of transport between the bud tip and neck (2 μm/minute; Figure 3) were consistent with a myosin-based motility mechanism [4] and the distribution of actin cables [27]. Maintenance at the bud cap was dependent upon two proteins, Bni1p/She5p and Bud6p/Aip3p, which define a cortical scaffold for anchoring mRNA and other polarized determinants in the bud.

Sequences located in the 3′UTR of *ASH1* are sufficient to direct an RNA transcript into the bud (Figures 2,3 and Supplementary material) [3,14–16]. Recent evidence indicates, however, that additional *cis*-acting elements within the coding region of *ASH1* contribute to localization of *ASH1* mRNA [15,16]. The $gRNA_{ASH1}$ reporter transcript described here includes a region that codes for the 27 carboxy-terminal amino acids of Ash1p together with the 3′UTR. Localization of the $gRNA_{ASH1}$ by this single element may be sensitized to perturbations in localization and/or anchorage of *ASH1* mRNA. This sensitized $gRNA_{ASH1}$ system has allowed identification of components, Bni1p/She5p and Bud6p/Aip3p, that maintain *ASH1* mRNA at the cortical bud cap. It is likely that redundant mechanisms in the coding region of *ASH1* mRNA or in Ash1p itself [15] stabilize the endogenous transcript in wild-type cells.

Bni1p/She1p and Bud6p/Aip3p participate in a number of polarity-driven pathways including actin organization [24,26], mating projection formation [25], and spindle orientation ([18,28,29]; C. Yang, P. Maddox, E. Chin, E. Yeh, E.D.S., D. Lew, and K.B., unpublished observations). Both Bni1p/She1p and Bud6p/Aip3p localize to regions of polarized cell growth [5,24] where they affect actin organization through direct connections to the actin cytoskeleton [24–26], and through mitogen-activated protein kinase pathways [24,25]. In addition, Bni1p/She5p and Bud6p/Aip3p may physically link actin and microtubules through Kar9p [18]. Kar9p orients cytoplasmic microtubules to maintain nuclear positioning in

Figure 9

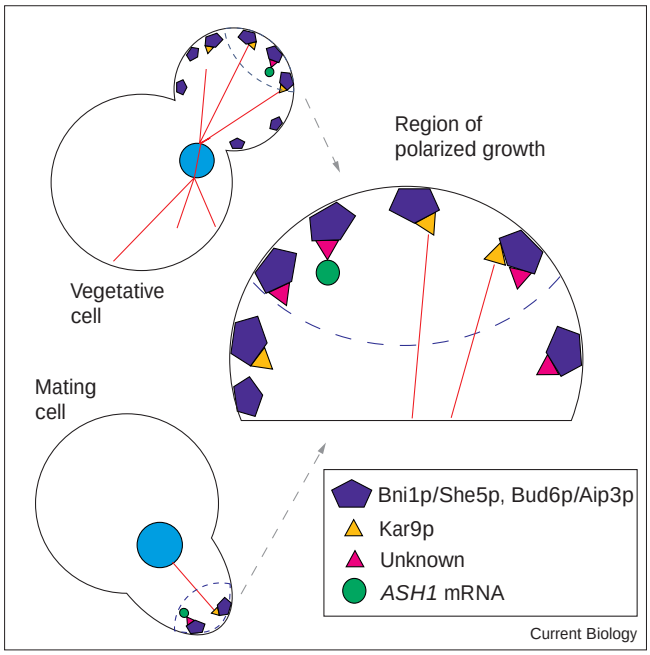

A generalized model of the cortical scaffold in regions of polarized cell growth. Within such a region (shown enclosed by a dashed dark blue line) at either the cortical bud cap in a vegetative cell or the mating projection tip, Bni1p/She5p and Bud6p/Aip3p (dark blue) act as a cortical attachment site for any molecules that are targeted for the bud. Targets, including at least microtubules (red) and *ASH1* mRNA (green), attach to the scaffold through effector proteins. The effector for microtubule binding is likely to be Kar9p (orange) [18], whereas the effector for the mRNA (pink) remains unknown. The nucleus is shown in light blue with a red mitotic spindle. Actin structures are excluded for clarity.

vegetative and mating cells [17]. Both Bni1p/She5p and Bud6p/Aip3p are required for localization of Kar9p at the tip of the bud in vegetative cells and the mating projection [18] (D.L.B., P. Maddox, J. Thibodeaux, and K.B., unpublished observations). The requirement for Bni1p/She5p and Bud6p/Aip3p in the localization of *ASH1* mRNA indicates that these proteins may form a generalized scaffold to maintain the orientation and positioning of factors between the mother and the bud.

Deletion of either *BNI1/SHE5* or *BUD6/AIP3* resulted in the release of $gRNA_{ASH1}$ from the cortical cap without affecting transport of the RNA between mother and bud (Figures 5,6). While some propensity for localization to the bud tip remained (Figures 6,7), $gRNA_{ASH1}$ moved throughout the bud in *bni1/she5* and *bud6/aip3* mutants and was even found to transiently foray into the body of the mother cell (data not shown). Additionally, $gRNA_{ASH1}$ was not associated with the incipient bud site in *bud6/aip3* cells and migration into the new bud was delayed by between 4 and 30 minutes after detectable bud growth (Figure 7). The velocities of these movements (0.467 μm/minute and 0.868 μm/minute for *bni1/she5* and *bud6/aip3*, respectively) were similar to the velocities reported for chromosome diffusion in *Saccharomyces cerevisiae* (0.1–1 μm/minute [30]). Sodium azide treatment, which arrests cell division and cortical actin patch movement by compromising cell metabolism [31], did not affect $gRNA_{ASH1}$ movement (D.L.B. and K.B., unpublished observations). Following actomyosin-dependent transport into the bud, the $gRNA_{ASH1}$ movement may reflect a diffusion-driven mechanism, rather than active transport.

Maintenance of the $gRNA_{ASH1}$ at the cortical cap is likely to result from interactions with a binding partner that is associated with a regional subset of the Bni1p/She5p and Bud6p/Aip3p that is present. Cell-cycle-dependent localization of $gRNA_{ASH1}$ mirrored that of Bud6p/Aip3p for vegetative [26] and mating cells [25]. During vegetative growth, Bud6p/Aip3p is distributed throughout the bud (Figure 8), whereas the $gRNA_{ASH1}$ remains at the bud tip (Figure 3a). An effector protein may facilitate mRNA interactions with a subset of the Bud6p/Aip3p–Bni1p/She5p scaffold at the cortical cap, analogous to the role of Kar9p as an effector between Bud6p/Aip3p–Bni1p/She5p and cytoplasmic microtubules (Figure 9) [18]. Whereas Kar9p mediates spindle orientation through Bni1p/She5p and Bud6p/Aip3p, we propose that an RNA-binding effector may mediate localization of *ASH1* mRNA to the same or similar scaffold (Figure 9).

The dependence of $gRNA_{ASH1}$ anchorage on Bni1p/She5p and Bud6p/Aip3p, and the colocalization of $gRNA_{ASH1}$ with Bud6p/Aip3p, coupled with similar spindle orientation defects in *bni1/she5* and *bud6/aip3* mutants, suggest roles for Bni1p/She5p and Bud6p/Aip3p in a multipurpose cortical scaffold that is active in both vegetative and mating cells (Figure 9). Interaction between specific molecules and the scaffold is mediated through individual effector molecules that act as adapters between the scaffold and the target (Figure 9). The scaffold functions to mediate the flow of information between the mother cell and either the bud or the shmoo tip by selective retention of polarized molecules such as *ASH1* mRNA or the plus ends of microtubules. We propose that this generalized cortical scaffold is positioned at regions of polarized cellular growth to facilitate maintenance of a polar axis and directional traffic between domains of the cell.

Materials and methods

Yeast strains

Wild-type strains 9D (*MATα, leu2, lys2, ura3, his3, ben*^{s}) [32] and YEF473A (*MAT**a**, trp1Δ63, leu2Δ1, ura3-52, his3-Δ200, lys2-801amber*) [26] were used throughout these experiments. A *myo4/she1::ura3* strain was constructed by fragment-mediated transformation using YCplacIII [5] cut with *Nhe*I to replace the *MYO4/SHE1* coding region with *URA3* in strain 9D. The *URA3* marker was then counter selected on 5-fluoroorotic acid (FOA) so that we could obtain a *ura3*, *myo4/she1* strain (9D *myo4/she1::ura3*). Strain YEF473A was transformed with a PCR-generated fragment to replace the

BNI1/SHE5 coding region with that of *LEU2*. Primers BNI1f (5′-GCCATTTGTATCTATCTTCTGTATTGAGGAGAAACATTTTAA-CTCAAGCCTAGTTAAATTCTAAATACACGCCGATTGTACTGAGA-GTGCACC-3′) and BNI1r (5′-GATGTTTGTTTTGGTATTACTGTT-GTCATAATTTTTTGGTTTAATATTTTATTTGAAACTTAGCCTGTTAC-CTGTGCTATGCGGTATTTCACACCG-3′) were used to amplify the *LEU2* region of pRS305 [33], generating a fragment for transformation-mediated deletion of the *BNI1/SHE5* coding region. Both the *myo4/she1::ura3* and the *bni1/she5::LEU2* deletions were verified by PCR using primers flanking the wild-type coding region. To image Bud6p/Aip3p localization in cells, YEF473A cells were transformed with pDAB204, a centromere-containing plasmid expressing the Bud6p/Aip3p–GFP fusion from the actin promoter (obtained from John Pringle). Cells were imaged as described below.

Media

Wild-type cells were grown in YPD (2% glucose, 1% yeast extract, 2% peptone). Cells transformed with plasmids pCP–GFP and pIIIA derivatives (see below) were grown on selective synthetic glucose (SD)-based media lacking uracil and histidine (SD–URA–HIS: 0.67% yeast nitrogen base, 2% glucose). To induce CP–GFP production, cells were switched to YNB+LEU+LYS (0.67% yeast nitrogen base, 2% glucose, 180 μg/ml leucine, and 90 μg/ml lysine) for 1–2 h. FOA media was SD-complete media (0.67% yeast nitrogen base, 2% glucose, 0.5% casamino amino acids, 50 μg/ml uracil, 50 μg/ml tryptophan, 50 μg/ml adenine) supplemented with 1 mg/ml 5-FOA. To induce mating projection formation in *MAT***a** cells, the appropriate media was supplemented with 50 μM α factor.

Expression plasmid construction

The CP–GFP fusion was expressed from the plasmid pCP–GFP. The coding region of the CP was subcloned by PCR from pCT119 [34] into the yeast expression plasmid pUG23 [35] upstream of the GFP coding region. Primers used to amplify CP were CP-FOR: 5′-GCTTGCATGC-CTGCAGGTCG-3′ and CP2BAM-R: 5′-GCGGATCCGTAGATGC-CGGAGTTTG-3′. For subcloning, a *Bam*HI site was engineered into the 3′ end of the PCR fragment, and an endogenous *Xba*I site upstream of the coding region was included in the amplified region. The digested PCR fragment was ligated between the *Xba*I and *Bam*HI sites within the polylinker of pUG23. The reading frame between the CP and GFP coding regions was maintained, and included an 18 amino acid spacer. This strategy produced pCP–GFP, a low-copy, *HIS3*-selectable, centromere-containing plasmid that produced CP–GFP regulated by the *MET25* promoter. Cells grown in the presence of methionine produced no detectable CP–GFP protein product, as determined by fluorescence signal intensity from imaged cells. Induction of the *MET25* promoter by methionine starvation produced a time-dependent increase in the fluorescence levels that were observed in individual cells (data not shown). The amount of fluorescence varied between individual cells within the population [36] and was distributed throughout the cytoplasm and excluded only from the vacuole.

RNA expressed from pIIIA/MS2-1 contains two tandem copies of the CP-binding site. The plasmid was used to produce a nuclear RNA transcript containing the binding sites for the MS2 coat protein flanked by the RNAseP leader and termination sequences ($gRNA_{NUC}$) [37]. Constitutive transcription by RNA polymerase III is driven by the RNAse P promoter.

To produce an asymmetrically localized RNA, we combined the CP-binding site and the *ASH1* 3′UTR. The *Eco*RI–*Sca*I fragment from pAS174 [1] containing the *ASH1* 3′UTR was treated with the Klenow fragment of DNA polymerase and ligated into the *Sma*I site of pIIIA/MS2-1 [37]. The 581 bp fragment excised from pAS174 included the entire UTR between *ASH1* and the next adjacent reading frame (*SPE1*), encompassing a region known to direct localization of an mRNA transcript [3,14]. This produced two plasmids containing the inserted 3′UTR in either orientation downstream from the tandem CP-binding sites: pIIIA/UTR and pIIIA/UTRop. Each of these 2 μ plasmids expressed a transcript from the ubiquitous RNA polymerase III promoter. The coding region of this transcript includes an RNAse P leader sequence, tandem CP-binding sites, the *ASH1* 3′UTR (forward orientation: $gRNA_{ASH1}$, reverse orientation: $gRNA_{NONCODING}$), and the RNAse P transcription terminator.

We used a similar strategy to produce a transcript containing the *KAR9* 3′UTR. A DNA fragment containing the *KAR9* 3′UTR was generated by PCR from genomic DNA of strain 9D. Primers used for this PCR were K9UTR-up: 5′-AAGGCCTAAGGGCGTTTAGATAAAACC-3′ and K9UTR-dn: 5′-AAGGCCTCTTATAAAATCTAAAGCATCATCC-3′. The fragment generated by PCR included the final 10 amino acids of *KAR9*, the entire intergenic region (272 bp), and the first 29 amino acids of the adjacent coding region. Including *Stu*I sites in the primers allowed ligation of the fragment into the pIIIA/MS2-1 *Sma*I site to produce pIIIA/K9UTR and pIIIA/K9UTRop. These plasmids ubiquitously express the CP-binding site fused to the *KAR9* 3′UTR in either orientation (forward orientation: $gRNA_{KAR9}$, reverse orientation: $gRNA_{KAR9\text{-}NC}$).

Expression by the constitutive RNA polymerase III promoter maintained RNA levels throughout the cell cycle. Overproduction of the RNA did not affect cell morphology, doubling time, bud-site selection (haploid or diploid), or kinetics of nuclear separation (see Results).

Velocity measurements

RNA velocity measurements were obtained by measuring the point-to-point movements of $gRNA_{ASH1}$ spots. The distance of spot movements at 1 or 2 min intervals provided instantaneous velocities representing a minimal speed at each timepoint. Because the spots frequently change direction between time points, continuous velocities could not be measured. Maximal speeds were measured when the $gRNA_{ASH1}$ traversed the entire cell, such as from the bud tip to neck. Because accurate sustained velocities could not be recorded, we report the range of instantaneous velocities for $gRNA_{ASH1}$ spot movements.

Fluorescence in situ *hybridization*

FISH was performed as described by Takizawa *et al.* (http://motorhead.ucsf.edu/valelab/res-rna-transprot.html) [14]. Alterations to the protocol included fixation for 2 h in 4% formaldehyde, and the use of a DNA probe. A 291 bp probe complementary to the 5′ region of the gRNA transcript from pIIIA/UTR was generated by PCR and labeled using the PCR digoxigenin (DIG) Probe Synthesis Kit (Boehringer Mannheim). Primers used to generate the fragment were 5′-GAAAGAA-GAGATTCAGTTATCCATG-3′ and 5′-TTACGTTTGAGGCCTCGTG-3′. The DIG-labeled DNA probe was denatured by boiling for 5 min before addition to the hybridization buffer. The probe was detected using alkaline-phosphatase-conjugated anti-DIG Fab fragments (Boehringer Mannheim) and HNPP fluorescent substrate with Fast Red (Boehringer Mannheim), and imaged using a rhodamine filter set.

Microscopy and image processing

Microscopy and digital imaging was performed as described by Shaw *et al.* [13,32]. Images were generated using a Hamamatsu Orca (Model C4742-95) digital camera and either a Nikon Optiphot using a 60× 1.4 NA Plan Apochromat objective and 1.25× magnification to the camera or a Nikon Eclipse E600FN using 100× 1.4 NA Plan Apochromat objective with 1× magnification to the camera. Single-image planes were taken instead of using optical sectioning, and oblique-illumination bright-field imaging replaced DIC.

We used the 3D Reconstruction feature of the Metamorph software package (Universal Imaging Corporation) to generate a composite image of several time points (Figure 6). The function controls were set to create a single image with 0° of rotation of a projection of the brightest points from a sequence of images. This produced a time-lapse composite image representing the distribution of the $gRNA_{ASH1}$ over a period of time.

Supplementary material

A supplementary figure showing the localization by FISH of $gRNA_{ASH1}$ in the absence of CP–GFP is published with this article on the internet.

Acknowledgements

We thank Paul Maddox and Elaine Yeh for helpful comments and critical reading of the manuscript, Julie Thibodeaux and Susan Whitfield for technical assistance, David Peabody (University of New Mexico) for the generous gift of the MS2 coat protein cDNA (pCT119), and John Pringle (University of North Carolina at Chapel Hill) for mutant strains. D.L.B. would like to express his appreciation for encouragement given by Ann Lyke, Paul Maddox, Julie Conman, and Amy Shaub. National Institutes of Health grants GM32238 issued to K.B. and GM24364 issued to E.D.S. supported this work.

References

1. Sil A, Herskowitz I: Identification of asymmetrically localized determinant, Ash1p, required for lineage-specific transcription of the yeast HO gene. *Cell* 1996, 84:711-722.
2. Bobola N, Jansen R-P, Shin TH, Nasmyth K: Asymmetric accumulation of Ash1p in postanaphase nuclei depends on a myosin and restricts yeast mating-type switching to mother cells. *Cell* 1996, 84:699-709.
3. Long RM, Singer RH, Meng X, Gonzalez I, Nasmyth K, Jansen R-P: Mating type switching in yeast controlled by asymmetric localization of ***ASH1*** mRNA. *Science* 1997, 277:383-387.
4. Bertrand E, Chartrand P, Schaefer M, Shenoy SM, Singer RH, Long RM: Localization of ***ASH1*** mRNA particles in living yeast. *Mol Cell* 1998, 2:437-445.
5. Jansen R-P, Dowzer C, Michaelis C, Galova M, Nasmyth K: Mother cell-specific ***HO*** expression in budding yeast depends on the unconventional myosin Myo4p and other cytoplasmic proteins. *Cell* 1996, 84:687-697.
6. Singer RH: RNA zipcodes for cytoplasmic addresses. *Curr Biol* 1993, 3:719-721.
7. Deshler JO, Highett MI, Abramson T, Schnapp BJ: A highly conserved RNA-binding protein for cytoplasmic mRNA localization in vertebrates. *Curr Biol* 1998, 8:489-496.
8. Ainger K, Avossa D, Morgan F, Hill SJ, Barry C, Barbarese E, *et al.*: Transport and localization of exogenous myelin basic protein mRNA microinjected into oligodendrocytes. *J Cell Biol* 1993, 123:431-441.
9. Knowles RB, Sabry JH, Martone MA, Ellisman M, Bassell GJ, Kosik KS: Translocation of RNA granules in living neurons. *J Neurosci* 1996, 16:7812-7820.
10. Peabody DS: Translational repression by bacteriophage MS2 coat protein expressed from a plasmid. *J Biol Chem* 1990, 265:5684-5689.
11. Stripecke R, Oliveira CC, McCarthy JEG, Hentze MW: Proteins binding to 5′ untranslated region sites: a general mechanism for translational regulation of mRNAs in human and yeast cells. *Mol Cell Biol* 1994, 14:5898-5909.
12. Yeh E, Skibbens RV, Cheng JW, Salmon ED, Bloom K: Spindle dynamics and cell cycle regulation of dynein in the budding yeast, ***Saccharomyces cerevisiae***. *J Cell Biol* 1995, 130:687-700.
13. Shaw SL, Yeh E, Bloom K, Salmon ED: Imaging green fluorescent protein fusion proteins in ***Saccharomyces cerevisiae***. *Curr Biol* 1997, 7:701-704.
14. Takizawa PA, Sil A, Swedlow JR, Herskowitz I, Vale RD: Actin-dependant localization of an RNA encoding a cell-fate determinant in yeast. *Nature* 1997, 389:90-96.
15. Gonzalez I, Buonomo SBC, Nasmyth K, Von Ahsen U: ***ASH1*** mRNA localization in yeast involves multiple secondary structural elements and Ash1 protein translation. *Curr Biol* 1999, 9:337-340.
16. Chartrand P, Meng X-H, Singer RH, Long RM: Structural elements required for the localization of ***ASH1*** mRNA and of a green fluorescent protein reporter particle ***in vivo***. *Curr Biol* 1999, 9:333-336.
17. Miller RK, Rose MD: Kar9p is a novel cortical protein required for cytoplasmic microtubule orientation in yeast. *J Cell Biol* 1998, 140:377-390.
18. Miller R, Matheos D, Rose M: The cortical localization of the microtubule orientation protein, Kar9p, is dependent upon actin and proteins required for polarization. *J Cell Biol* 1999, 144:963-975.
19. Byers B: Cytology of the yeast life cycle. In *The Molecular Biology of the Yeast* Saccharomyces*: Life Cycle and Inheritance.* Edited by Strathern JN, Jones EW and Broach JR. Cold Spring Harbor, New York: Cold Spring Harbor Laboratory; 1981:59-96.
20. Chant J: Generation of cell polarity in yeast. *Curr Opin Cell Biol* 1996, 8:557-565.
21. Erdman S, Lin L, Snyder M: Pheromone-regulated genes required for yeast mating differentiation. *J Cell Biol* 1998, 140:461-483.
22. Pringle JR, Bi E, Harkins HA, Zahner JE, De VC, Chant J, *et al.*: Establishment of cell polarity in yeast. *Cold Spring Harb Symp Quant Biol* 1995, 60:729-744.
23. Haarer BK, Petzold A, Lillie SH, Brown SS: Identification of MYO4, a second class V myosin gene in yeast. *J Cell Sci* 1994, 107:1055-1064.
24. Fujiwara T, Tanaka K, Mino A, Kikyo M, Takashi K, Shimizu K, *et al.*: Rho1p-Bni1p-Spa2p interactions: implication in localization of Bni1p at the bud site and regulation of the actin cytoskeleton in ***Saccharomyces cerevisiae***. *Mol Biol Cell* 1998, 9:1221-1233.
25. Evangelista M, Blundell K, Longtine MS, Chow CJ, Adames N, Pringle JR, *et al.*: Bni1p, a yeast formin linking Cdc42p and the actin cytoskeleton during polarized morphogenesis. *Science* 1997, 276:118-122.
26. Amberg DC, Zahner JE, Mulholland JW, Pringle JR, Botstein D: Aip3p/Bud6p, a yeast actin-interacting protein that is involved in morphogenesis and the selection of bipolar budding sites. *Mol Biol Cell* 1997, 8:729-753.
27. Kilmartin JV, Adams EM: Structural rearrangements of tubulin and Actin during the cell cycle of the yeast ***Saccharomyces***. *J Cell Biol* 1984, 98:922-933.
28. Lee L, Klee SK, Evangelista M, Bonne C, Pellman D: Control of mitotic spindle position by the ***Saccharomyces cerevisiae*** formin Bni1p. *J Cell Biol* 1999, 144:947-961.
29. Heil-Chapdelaine RA, Adames NR, Cooper JA: Formin′ the connection between microtubules and the cell cortex. *J Cell Biol* 1999, 144:809-811.
30. Marshall WF, Straight A, Marko JF, Swedlow J, Dernberg A, Belmont L, *et al.*: Interphase chromosomes undergo constrained diffusional motion in living cells. *Curr Biol* 1997, 7:930-939.
31. Doyle T, Botstein D: Movement of yeast cortical actin cytoskeleton visualized ***in vivo***. *Proc Natl Acad Sci USA* 1996, 93:3886-3891.
32. Shaw SL, Yeh E, Maddox P, Salmon ED, Bloom K: Astral microtubule dynamics in yeast: a microtubule-based searching mechanism for spindle orientation and nuclear migration into the bud. *J Cell Biol* 1997, 139:985-994.
33. Christianson TW, Sikorski RS, Dante M, Shero JH, Hieter P: Multifunctional yeast high-copy-number shuttle vectors. *Gene* 1992, 110:119-122.
34. Lim F, Peabody DS: Mutations that increase the affinity of a translational repressor for RNA. *Nucleic Acids Res* 1994, 22:3748-3752.
35. Niedenthal RK, Riles L, Hegeman JH: Green fluorescent protein as a marker for gene expression and subcellular localization in budding yeast. *Yeast* 1996, 12:773-786.
36. Bloom K, Beach DL, Maddox P, Shaw SL, Yeh E, Salmon ED: Using green fluorescent protein fusion proteins to quantitate microtubule and spindle dynamics in budding yeast. In *Methods in Cell Biology*. Edited by Reider C. San Diego: Academic Press; 1998:369-383.
37. SenGupta DJ, Zhang B, Kraemer B, Pochart P, Fields S, Wickens M: A three-hybrid system to detect RNA-protein interactions in vivo. *Proc Natl Acad Sci USA* 1996, 93:8496-8501.

Because *Current Biology* operates a 'Continuous Publication System' for Research Papers, this paper has been published on the internet before being printed. The paper can be accessed from http://biomednet.com/cbiology/cub – for further information, see the explanation on the contents page.

Supplementary material

Localization and anchoring of mRNA in budding yeast

Dale L. Beach, E.D. Salmon and Kerry Bloom

Current Biology 19 May 1999, 9:569–578

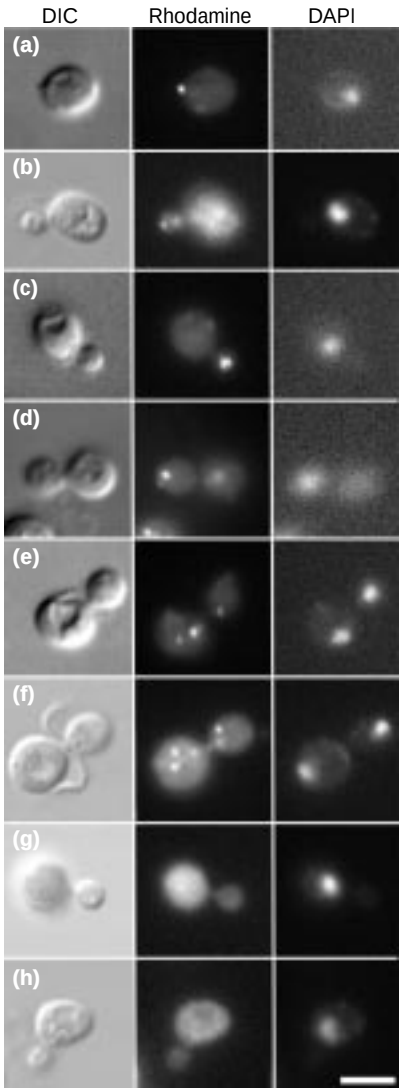

Current Biology

Figure S1

Localization of $gRNA_{ASH1}$ in fixed cells by FISH in the absence of CP–GFP. Three images of each cell are shown: DIC to display cell morphology, rhodamine to display $gRNA_{ASH1}$ transcript localization and DAPI to show nuclear morphology. (**a**) A cell with a small bud (facing left) contains $gRNA_{ASH1}$ filling the bud. (**b–d**) Cells with larger buds contain $gRNA_{ASH1}$ at or near the bud tip as single or multiple spots. The $gRNA_{ASH1}$ resides at the bud tip both before (b,c) and after (d) anaphase. (**e**,**f**) The $gRNA_{ASH1}$converges at the neck in cells after anaphase and before cell separation. (**g**,**h**) YEF473 cells that have not been transformed with the plasmid pIII/UTR; $gRNA_{ASH1}$ is not detected by FISH in these cells. The scale bar represents 5 μm.